

© 2012 Honeywell International Inc. subject to license to IMAPS. Reprinted, with permission, from Brett Clark, The Distribution and Transport of Alpha Activity in Tin, September, 2012.

This material is posted here with permission from IMAPS. Such permission does not in any way imply IMAPS endorsement of any of Honeywell International Inc.'s products or services.

The Distribution and Transport of Alpha Activity in Tin

Brett M. Clark,
Honeywell Electronic Materials
Spokane Washington 99216
(509) 252-8716 (509) 252-2100 fax Brett.Clark@Honeywell.com

Abstract

The presence of alpha emitters in packaging materials pose an increased risk to device reliability as device size decreases and flip chip and 3-D packaging technology becomes more widespread. Particularly troubling is the observation that alpha emission increases over time in some reported instances. Several experiments were conducted to examine alpha flux behavior in tin materials and determine the cause for the temporal alpha emissivity increase. The experiments determined the distribution of the alpha emitters within the material volume, and a mechanism based on microsegregation is presented to explain the non uniform distribution. Data describing differential isotope distribution within tin are also presented, providing confirmation of ^{210}Po transport within a solid tin matrix. The effects of microsegregation and ^{210}Po migration on alpha emissivity over time will be discussed. Potential impacts from these mechanisms on alpha emissivity in packaging applications will also be presented.

Key words: soft errors, alpha emissivity, microsegregation, polonium diffusion

Introduction

The issue of soft error reliability and the contribution of alpha emitting isotopes to single-event upsets (SEU) have been studied over the past decade.^{1,2} Initial research focused on Pb based solders used in semiconductor packaging and efforts to improve purity, particular with respect to alpha emitting isotopes.³ The transition to Pb free materials has shifted focus to tin based materials. In general, radioactivity decreases over time in materials not exposed to nuclear reactor conditions. However, several examples where alpha emission increases significantly have been observed in lead based materials.^{3,4} Alpha emissivity increasing over time increases SEU risk in devices sensitive to alpha induced upsets.⁴ Furthermore, the proximity of emitters with respect to sensitive node can have a significant impact on SEU.

Alpha emitting isotopes are present in the packaging materials at parts per billion concentrations and below.⁵ This paper will focus on the contribution of these trace elements, particularly the uranium decay chain daughter ^{210}Po . One common explanation for increasing alpha emissivity revolves around the disturbance of $^{210}\text{Pb}/^{210}\text{Po}$ secular equilibrium, and subsequent re-establishment of secular equilibrium with a resultant increase in alpha

flux.⁶ Some experimental data reported for Pb materials follow this mechanism,⁴ while other reported data departs from the behavior predicted.³ No comparable time dependant alpha emissivity data has been reported for tin materials. With Sn based materials becoming the preferred alternative to Pb, determining the temporal alpha emission characteristics of Sn is necessary. Several experiments were carried out to assess distribution of alpha emitters in Sn and describe the factors influencing the time dependence of the observed alpha emissivity. This paper presents data describing changing alpha emissivity in tin and report a combination of mechanisms where alpha emission in a material may increase over time. Data presented demonstrate that alpha emitting isotopes are not uniformly and randomly distributed. We propose mechanisms for nonuniform distribution and alpha emissivity data characterizing the nonuniformity.

Experiment 1: Characterization of Microsegregation

Two experiments were performed to assess activity distribution in 99.99% pure tin used for lead-free solders. The first experiment involved three different tin samples. The three samples were chosen on the basis of differential increasing alpha emission rate. As displayed in Figure 1, Sample A showed no significant increase in alpha emissivity within

measurement uncertainty over a period of two years, while samples B and C showed increasing counts within several months of processing.

The sheets were etched in 70% by volume high purity distilled hydrochloric acid/30% CMOS grade nitric acid to remove surface material, and washed thoroughly with deionized water. Sheets were weighed before and after etching, and the depth of tin removed calculated assuming uniform dissolution from the surface. The final sample thickness agreed with the calculated value assuming initial thickness less etched material. Alpha flux measurements were performed using an Alpha Sciences 1950 gas proportional counter. Measurement protocols followed those recommended in JESD221.⁷ Multiple iterations of the procedure were done, measuring the alpha activity at each successive surface. The range of a 5.3 MeV alpha particle in Sn is 16.5 μm ,⁸ and at least this material depth was etched away at each step to remove the previous analytical volume.

Results and Discussion

The alpha emissivity versus the first 100 micrometers in depth is plotted in Figure 2. Sample A shows no significant change, while samples B and C

show significant increase. The increase is strongly linear versus depth within the initial 100 micrometers, with correlation coefficients of 0.98 and 0.99. The strong correlation across multiple samples suggests that the experimental protocol did not introduce significant variation with respect to alpha emitter contaminants. The emissivity increase versus depth scales with the differential surface alpha emissivity, namely $\Delta\alpha_C > \Delta\alpha_B > \Delta\alpha_A \approx 0$. These data suggest the emitter concentration gradient in the material is directly proportional to the surface alpha emissivity increase on the surface. The surface alpha emissivity for sample B increased by a factor a 5 over 15 months, while Sample C emissivity doubled.

The expected alpha emissivity versus time due to secular equilibrium is plotted in Figure 1 for samples B and C. These curves were generated by calculating the number of ²¹⁰Pb atoms per cm² needed to increase the alpha flux in the respective samples to the initial data points in the requisite time. No curve was calculated for sample A since negligible change was observed. Both sample B and C deviate significantly from secular equilibrium predictions, and an additional time dependent mechanism is required to explain the data.

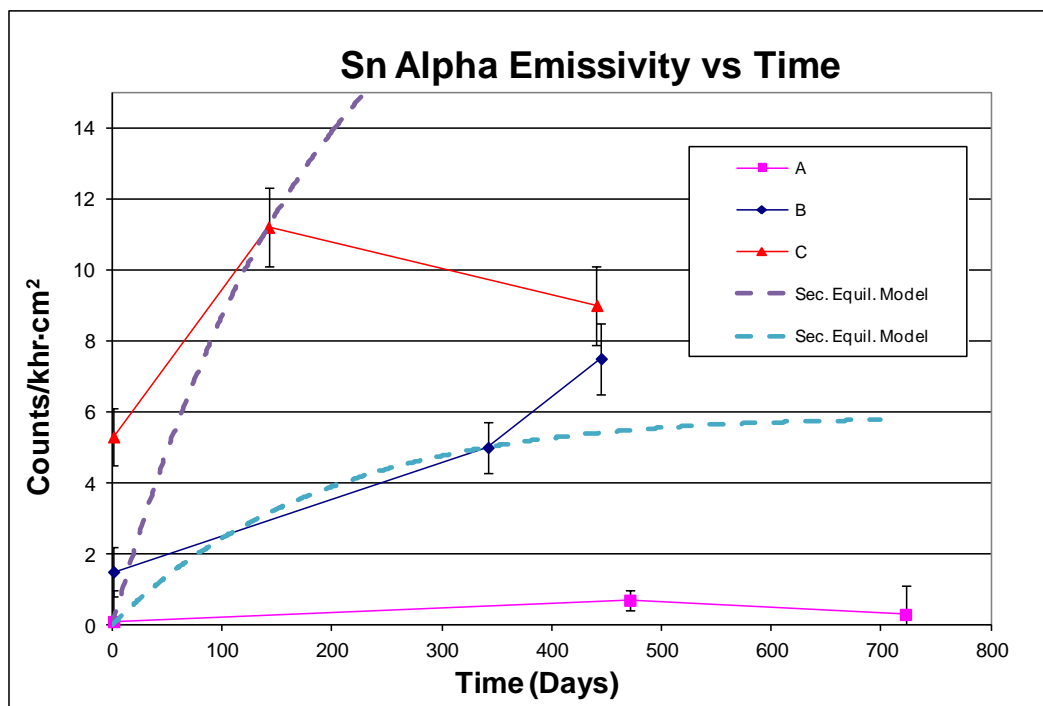


Figure 1. Alpha flux versus time for three Sn samples. One sigma error bars are shown.

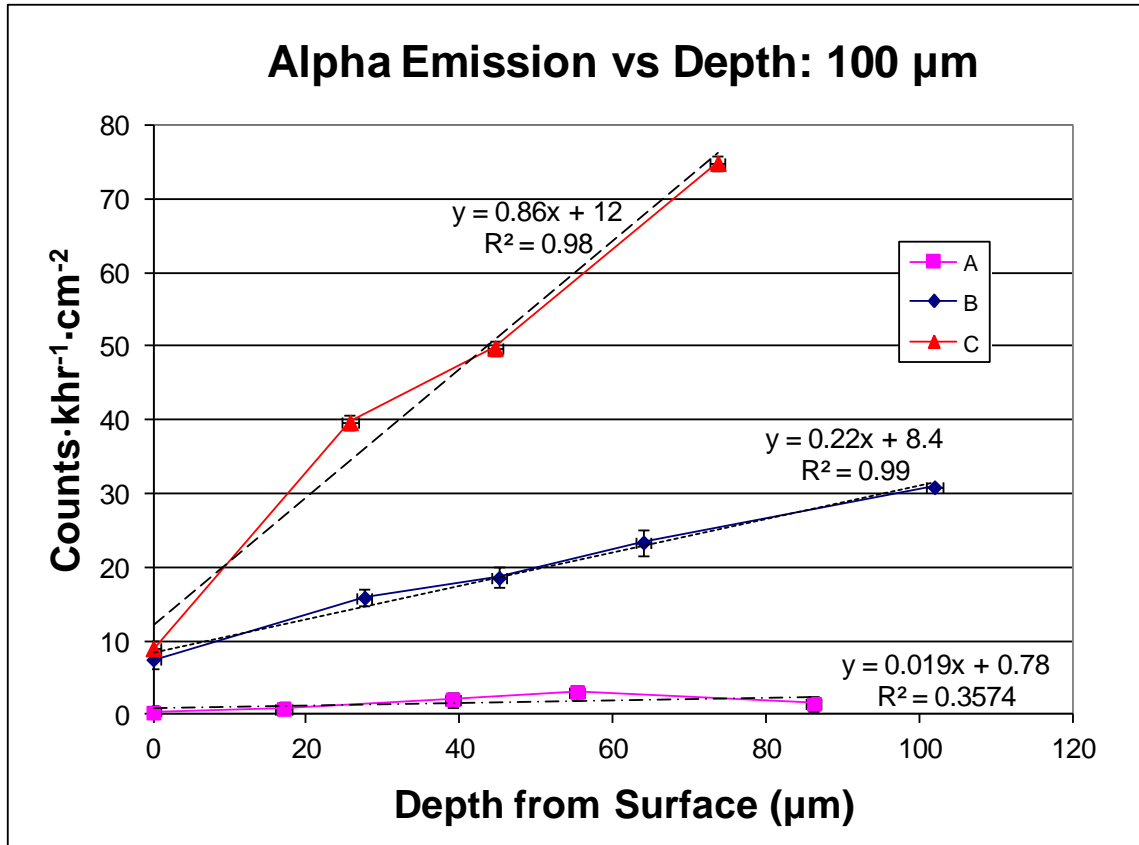


Figure 2. Alpha Emission versus 100 μm depth in three Sn samples.

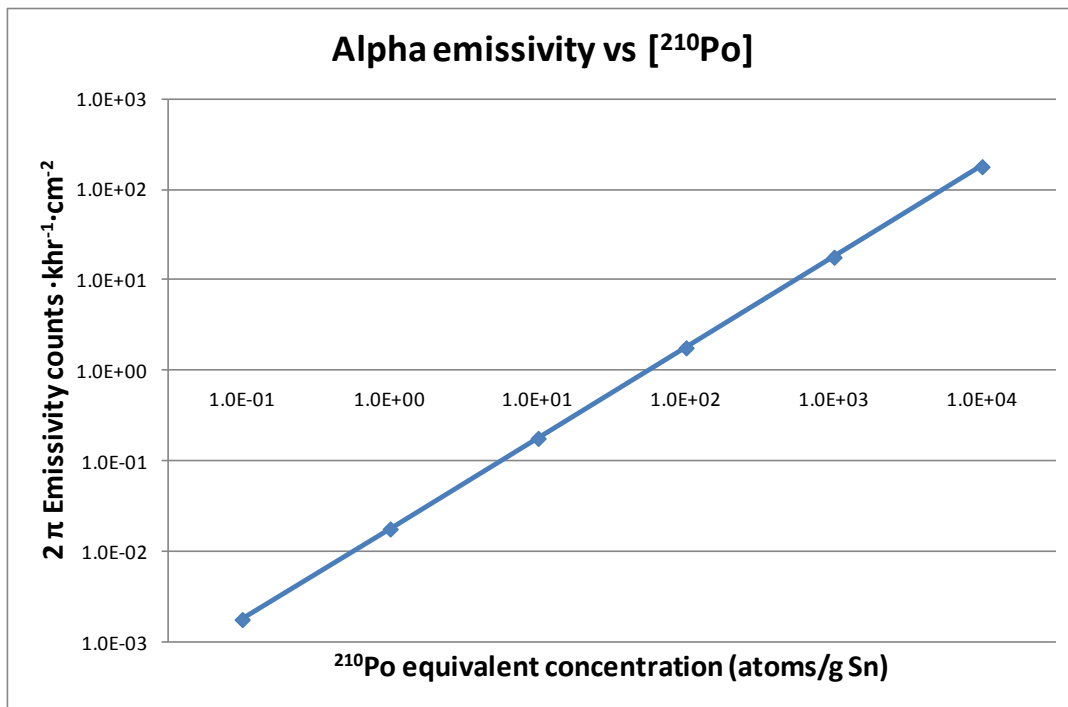


Figure 3. Theoretical alpha emissivity versus ²¹⁰Po concentration.

The distribution of alpha emitters within the material volume is explained by microsegregation, a well documented metallurgical phenomenon.⁹ Microsegregation arises in solid/liquid systems where solutes (e.g. alpha emitting isotopes) partition preferentially in the liquid phase versus the solid phase during solidification according to

$$k = \frac{C_S}{C_L} \quad (1)$$

where k is defined as the partition coefficient and C_S and C_L are the concentrations in the liquid and solid phases respectively. As solidification fronts propagate, solute concentration in the liquid phase increases if $k < 1$. The result is an elemental gradient along the solidification axis, with the largest solute concentration located in the final solidification volume. The gradient slope is a function of solidification rate and the solute concentration. Microsegregation is commonly observed in commercial alloys.¹⁰ One common technique employed to minimize microsegregation is rapid solidification. It should be noted that all three samples experienced comparable solidification conditions.

The different depth profiles of samples A, B, and C may be explained in terms of the concentration of alpha emitters within each. The higher the emitter concentration in the liquid phase, the larger amount partitions during solidification at each point within the depth according to equation 1, and the steeper the gradient. The ^{210}Po concentration equivalent to a

measured alpha flux $\epsilon_{\text{measured}}$ may be calculated from

$$[\text{Po}_\alpha](\text{ng} / \text{g}) = \frac{10^9 \epsilon_{\text{measured}} M}{\lambda N_A \rho A R f} \quad (2)$$

where λ is the decay reaction rate constant in hours, N_A is Avogadro's number, ρ is the density of the matrix in grams per mole, A is the measurement area in cm^2 , R is the alpha range in the matrix in centimeters (16 μm for the 5.3 MeV alpha), M is the molar mass of the emitter, and f is a geometric correction factor.³ Figure 3 shows the projected alpha emission as a function of polonium concentration assuming all the emission originates from Po. The maximum value of sample C in Figure 2 (74.9 $\alpha \cdot \text{km}^{-2} \cdot \text{hr}^{-1}$) corresponds to 1.5×10^{-18} grams of ^{210}Po per gram of Sn, or 4.2×10^3 ^{210}Po atoms per gram of Sn. The data suggest solute microsegregation is present several orders of magnitude below the parts per trillion (ppt) concentration range previously proposed for trace contamination.¹¹

While direct measurement of impurity concentration would be helpful, the analytical levels required are below current measurement capability. Glow Discharge Mass Spectrometry (GDMS) analysis of Sn failed to detect alpha emitting contaminants above 0.5 ppb detection limits. We therefore infer concentration changes from alpha radiation measurements.

The time dependence of alpha emissivity in Sn deviates from what is predicted by secular equilibrium. Nevertheless, the correlation between the concentration of impurities sequestered inside the material and emissivity change over time suggests a secondary mechanism is active.

Table 1. Data for alpha emissivity versus tin volume analyzed.

Sample Thickness	Sample Area (cm^2)	% Volume analyzed (both surfaces)	Bulk Alpha emissivity ($\alpha \cdot \text{cm}^{-2} \cdot \text{km}^{-1}$)			
			Side A	1 σ	Side B	1 σ
A	1800	4	17.2	0.7	14.8	0.6
B	1800	9	30.2	0.9	29.1	0.7
C	1800	19	36.1	0.9	32.4	0.9
D	1800	54	32.9	0.7	28.8	0.5

Experiment 2

A second experiment examined the alpha emitter distribution in a Sn ingot. The center portion of an ingot was removed and reduced to specific dimensions. The initial area of 900 cm^2 had an alpha emissivity of $18.4 \alpha \cdot \text{km}^{-1} \cdot \text{cm}^2$. The analytical volume of the measurement was 1.5 cm^3 , which

represents only 0.1 percent of the sample volume. After initial measurement, the sample was reduced to thinner dimensions and measured at each thickness. Both sides of the sample were measured to increase the effective volume measured at each iteration. Measurements were conducted using a XIA Ultra-L0 1800 ionization chamber, which has previously been used to study alpha emissivity.¹² The larger active

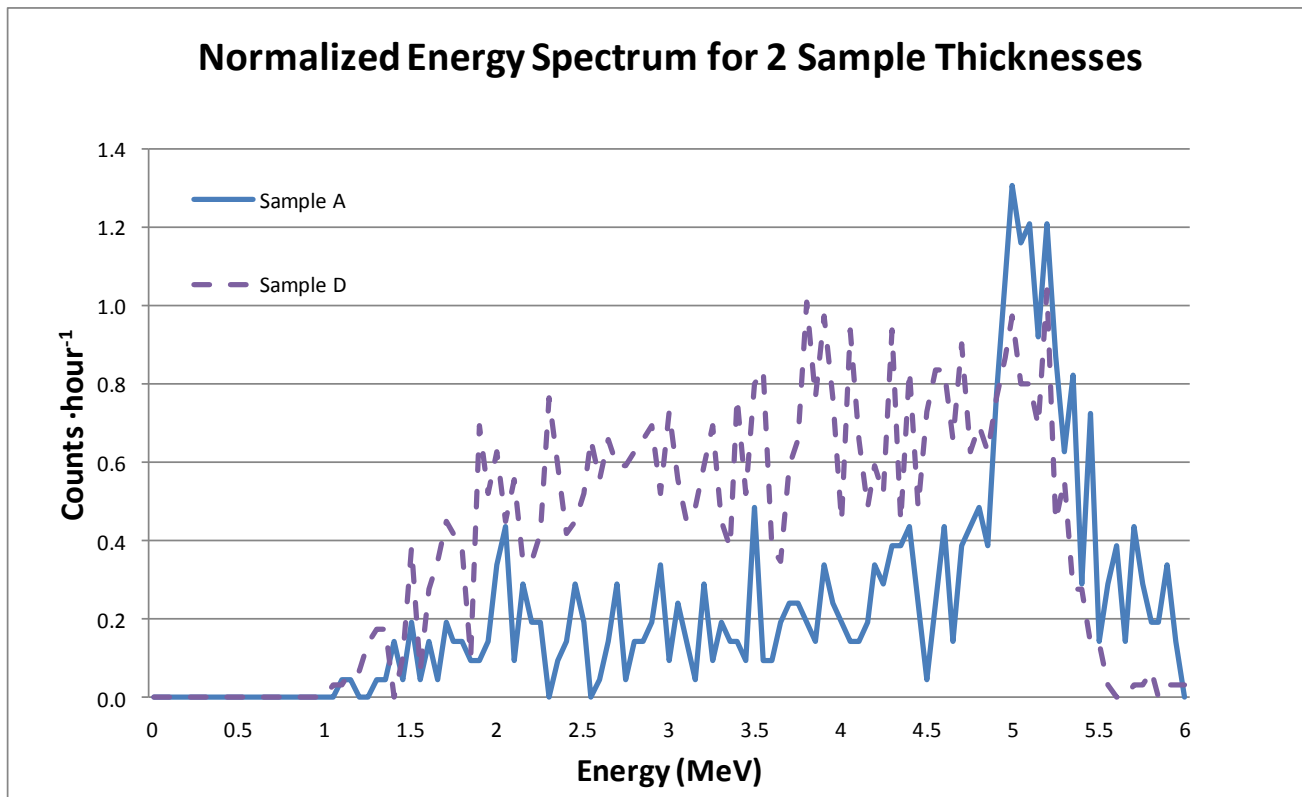


Figure 4. Energy spectra comparison

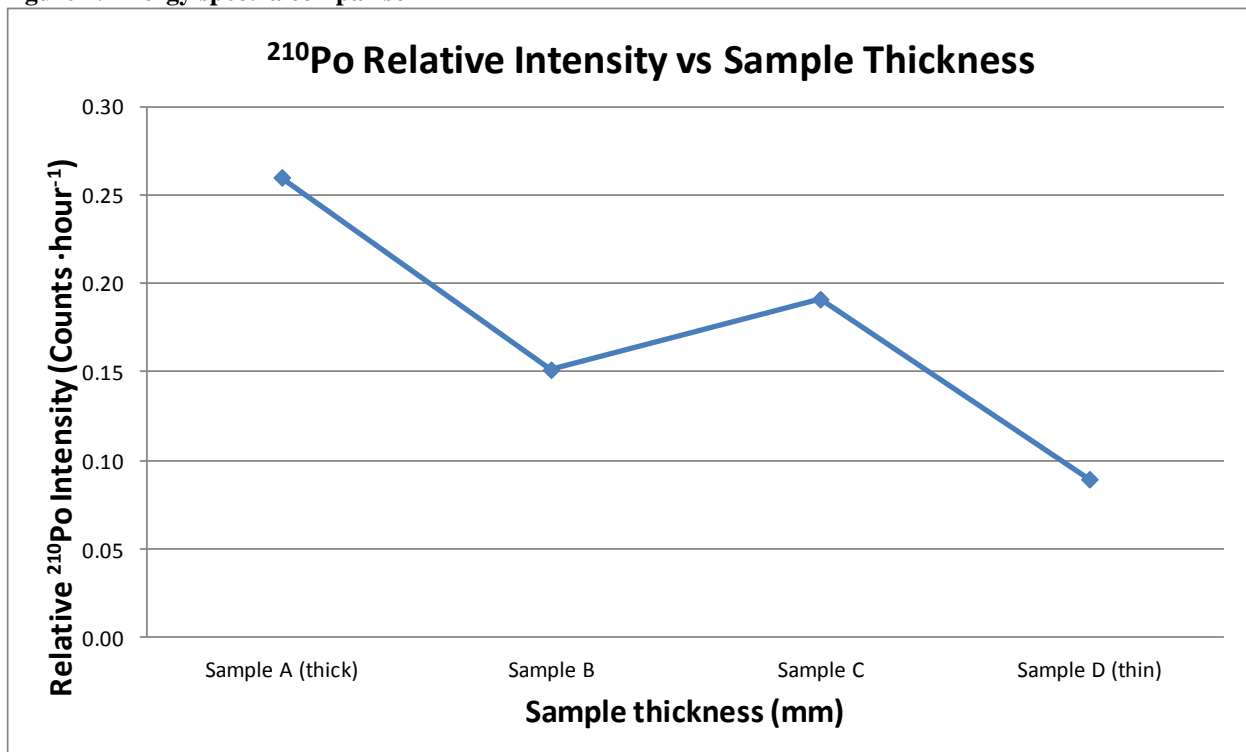


Figure 5. ²¹⁰Po relative surface emission versus sample thickness

area of this instrument enabled a greater volume of material to be analyzed, and the energy spectra generated enabled identification of the specific alpha emitting isotopes.

Results and Discussion

Table 1 contains the experimental parameters and the corresponding alpha emissivity data. The results show alpha emissivity increasing with decreasing sample thickness. These data are consistent with the observation in the previous experiment: that surface emissivity measurements significantly underestimate the thick sample emissivity where microsegregation effects are present. In addition, the emissivity from side A is statistically different from Side B. This may indicate one surface is closer to the final solidification zone than another.

The alpha spectrum was measured for both thick and thin samples and normalized to counting time. Differences in the alpha emission spectra (Figure 4) for sample thickness were observed. Sample A (thick) exhibited a pronounced surface ^{210}Po peak similar to surface emission from Sn solder bumps reported by Gordon.⁴ Sample D (thin) lacks prominent ^{210}Po emission but exhibits more emission in the 1-4.5 MeV range. This characteristic suggests that the emitting species are more concentrated subsurface than in the 0.81 thickness.

The ^{210}Po surface emissivity (5.1 – 5.6 MeV) relative to the total integrated counts from 1-8.5MeV for different thicknesses is plotted in Figure 5. For the 0.81 mm sample, ^{210}Po surface emission constitutes greater than 20% of the detected emissivity. The percentage hovers between 15 and 20% for intermediate thickness samples before dropping to less than 10 percent of the detected emissivity in 0.063 thick samples. The bulk activity increases by factor of 2 from the surface to interior, but the ^{210}Po component decreases by a comparable factor. These data support the hypothesis that ^{210}Po accumulates on the surface with a decreasing gradient into the material, and provide evidence that microsegregation is present in the ingot.

The experimental data presented above demonstrate that alpha emitting isotopes are not randomly distributed in the material undergoing liquid/solid phase transition. This hypothesis was earlier proposed by Clark.³ Typical metal manufacturing processes involve melting and solidification steps, during which alpha emitters may

be concentrated in the interior of the mass. Test samples made from solidification processes are expected to experience microsegregation effects. Alpha emissivity measurements conducted on samples thicker than the alpha escape range will yield an emissivity lower than the value for the entire volume when this mechanism is operable.

Experiment 3: Characterization of Diffusion

The observation of consistent ^{210}Po surface emission warranted further investigation to identify the source of this activity. ^{210}Po is a ^{222}Rn daughter, and atmospheric ^{222}Rn has been proposed as a potential Po source.⁶ An alternative explanation has been proposed by Zastawny, who reported Po surface enrichment in Pb by heating.¹³ In addition, Lykken described surface emission increasing with elevated sample temperature.¹⁴ Accordingly, an experiment was performed to determine the relative contributions to surface Po from the atmosphere and internal diffusion.

A 1,075 g mass of tin with emissivity of $2 \alpha \cdot \text{hr}^{-1} \cdot \text{cm}^{-2}$ was combined with an 11 g mass of 1910 $\alpha \cdot \text{hr}^{-1} \cdot \text{cm}^{-2}$ tin with a significant ^{210}Po surface emission (Figure 6). The two materials were melted in a graphite crucible and cast into a steel mold to form a 3 cm x 3 cm x 35 cm ingot. The ingot was cut in half, and both halves reduced to specific dimensions in preparation for alpha emissivity measurement. One half was used as the test sample, the other half served as a control sample. Both sample and control were measured within two weeks from the initial casting, with respective activities of $23.9 \pm 0.8 \alpha \cdot \text{hr}^{-1} \cdot \text{cm}^{-2}$ and $22.2 \pm 0.9 \alpha \cdot \text{hr}^{-1} \cdot \text{cm}^{-2}$. The test sample was oven heated at atmospheric pressure for 6 hours at 473K and placed in the ionization chamber within 20 minutes of removal from the oven. The emissivity was measured, and the control was measured within several days afterward. The test sample was then allowed to sit on clean room wipes on the lab bench adjacent to the oven for six hours at 294K, during which time the analyzed surface was face up and exposed to the atmosphere. The test sample was then re-measured, as was the control sample. The measurement/heat/measurement cycle was performed at 15, 45, 46, and 93 days from sample casting to assess the effect of temperature on alpha emissivity and Po distribution. The samples were stored in sealed polyethylene bags when not being heated or measured.

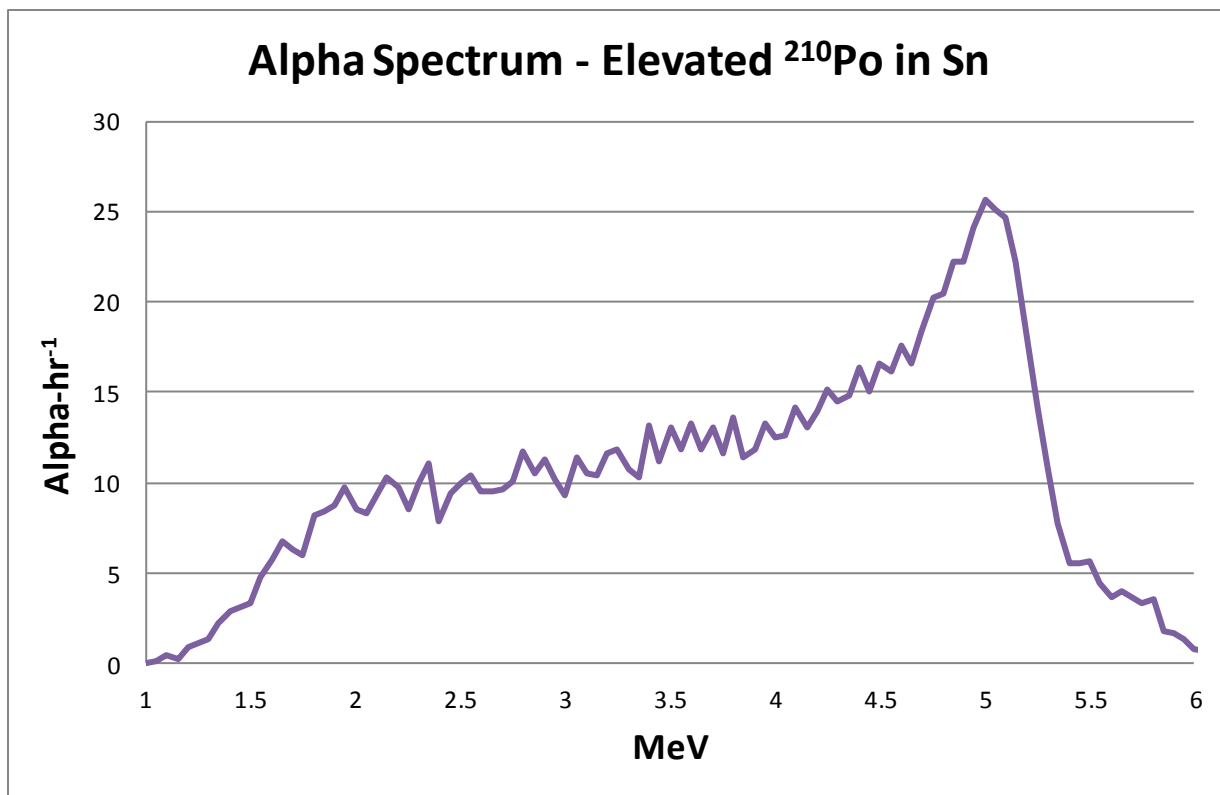


Figure 6. Alpha emission spectrum from Sn with elevated Po.

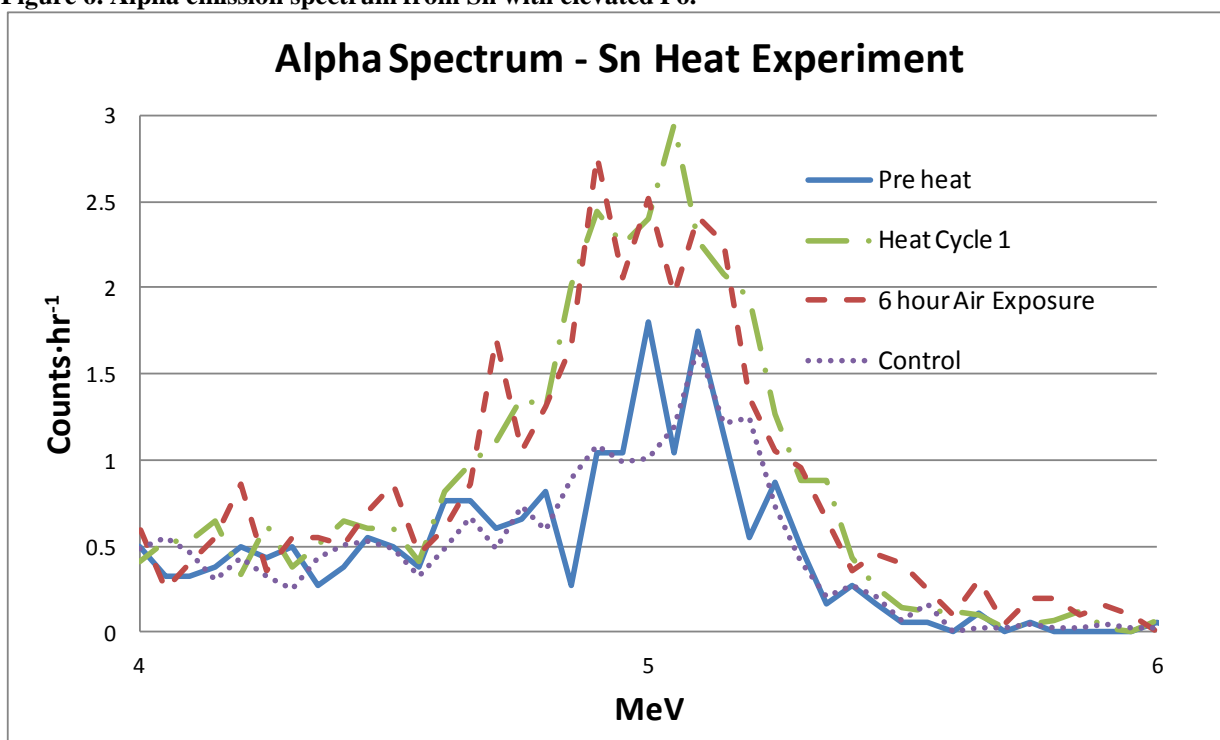


Figure 7. Normalized alpha spectra for test and control samples.

Table 2. Polonium Diffusion Experimental data

Test Sample			Control Sample		
Time Elapsed (days)	Bulk Emissivity $\alpha \cdot \text{KHR}^{-1} \cdot \text{CM}^{-2}$	^{210}Po Emissivity $\alpha \cdot \text{KHR}^{-1} \cdot \text{CM}^{-2}$		Bulk emissivity $\alpha \cdot \text{KHR}^{-1} \cdot \text{CM}^{-2}$	^{210}Po emissivity $\alpha \cdot \text{KHR}^{-1} \cdot \text{CM}^{-2}$
9	23.9 ± 0.8	4.6	12	22.2 ± 0.8	3.6
15	32.2 ± 0.7 [†]	8.6	16	22.8 ± 0.6	4.7
16	33.3 ± 0.9*	8.0	46	26.7 ± 0.9	6.5
45	29.5 ± 0.9	9.3	54	28.2 ± 0.9	7.7
46	33.4 ± 1.3 [†]	8.5	92	28.4 ± 1.0	8.8
47	33.6 ± 1.1 [†]	8.1			
92	32.1 ± 1.0	7.1			
93	34.2 ± 1.0 [†]	8.5			

*Represents Air test data

[†]Represents Post- Heating data

The normalized spectra for both test and control samples at each experimental step are shown in Figure 7. The initial spectrum shows a significant ^{210}Po peak at 5.3 MeV. After heating, alpha emissivity increased to 32.2 ± 0.7, and the integrated ^{210}Po peak intensity from 5.1 -5.5 MeV increased from 3.77 counts per hour per channel to 8.03 counts per hour per channel. After the 6 hour ambient exposure, the emissivity measured at 33.3 ± 1. The control sample activity was unchanged within measurement uncertainty (22.8 ± 0.7 versus 22.2 ± 0.9), whereas the test sample increased 38% after heat treatment. The air exposure caused the emission increase incrementally further, but the change is of the same order as the measurement uncertainty, making conclusive assignment of the cause difficult. Comparing the test and control sample results, and considering polonium diffusion is a function of temperature,¹⁵ it is reasonable to conclude that ^{210}Po activity predominately originated from within the sample.

An expression for the Po concentration in the analytical volume as a function of time may be written as:

$$[Po]_{\text{Surface}}(t) = \frac{\lambda_{Pb}}{\lambda_{Po} - \lambda_{Pb}} [^{210}Pb]_0 (e^{-\lambda_{Pb}t} - e^{-\lambda_{Po}t}) + J_{Po} \quad (3)$$

Where λ_{Pb} and λ_{Po} are decay constants and

$$J = -D \frac{\partial \phi_{Po}}{\partial x} \quad (4)$$

Equation 3 assumes negligible initial Po in the material. The first term reflects the contribution from secular equilibrium, and the second term represents the polonium diffusion contribution. The Po concentration, and by extension the emissivity, may vary in time depending on which term dominates.

Historical assumptions considered only the first term when assessing alpha emissivity versus time. The diffusion term dominates in elevated temperature conditions, while secular equilibrium influence becomes significant when diffusion slows at room temperature.

The total integrated emission from 1-9.5 MeV was plotted versus time in Figure 8, and associated data are tabulated in Table 2. The pre-heat measurement of the second test cycle revealed a 13 % decrease in the bulk alpha emissivity from 29 days earlier. These data suggest that after initial surface enrichment from elevated temperature diffusion, contributions from secular equilibrium and diffusion are room temperature are insufficient to sustain the surface Po concentration. The second heat cycle returned alpha flux to the same level measured after the air test. An additional heat cycle 1 day later did not change the emissivity within measurement error. This observation suggests that heating the Sn sample at 473 K for six hours is sufficient to drive essentially all the polonium in the sample to the surface, and additional heating yields no additional Po. The fourth heat cycle initial measurement is 5% lower than the previous measurement. This suggests a decrease in the number of decays depleting Po, an increase in Po from secular equilibrium and diffusion, or a combination of the two.

The control sample data in Figure 8 shows a linear ($R^2 = 0.99$) increase over the initial 54 days at a rate of 0.0001 $\alpha \cdot \text{KHR}^{-1} \cdot \text{CM}^{-2}$ per day. However, between 54 days and 96 days there is no change in the bulk emissivity. The departure from the linear trend is not understood at this juncture, but is potentially related to emitter position within the volume. It is expected that the plots for the control and test samples will intersect as secular equilibrium determines the temporal alpha characteristics in the absence of temperature drive diffusion.

The surface emission increase of lead sheets was attributed to polonium migration driven by a lower free energy state at the surface relative to the bulk.¹³ The data presented above support extending this hypothesis to tin. The surface ²¹⁰Po emission from Sn solder bumps reported by Gordon⁴ could also be explained by this mechanism.

The surface activity was estimated assuming alphas with energies in the interval 5.0-5.6 MeV originated from the sample surface and did not lose appreciable energy in matrix interactions. The range is broad due of the energy resolution limitations of the XIA instrument.⁴ The integrated ²¹⁰Po counts per hour were determined (see Table 2), and the number of ²¹⁰Po atoms *N* on the surface calculated from

$$N = \frac{At_{1/2}}{\ln 2f} \quad (4)$$

where *t*_{1/2} is the half life of ²¹⁰Po (3321 hours) and *f* is the geometric factor from equation 2. For the first heating cycle, the change in the number of moles on the 1800 cm² tin surface is calculated to be 1.8x10⁻¹⁹ mol. Adjusting for sample area and heating time, the ²¹⁰Po diffusion is calculated to be 4.5x10⁻²³ mol·m⁻²·s⁻¹ at 473K. Given that the diffusion occurred over a 6 hour period, this is a lower bound on the diffusion rate. Additional experiments utilizing shorter heating intervals will enable more accurate quantification of the diffusion rate. The diffusion rate at 293 K calculated from the control sample data over the linear 54 day period is 2x10⁻²³ mol·m⁻²·s⁻¹. Increasing the temperature 180° increased the diffusion rate by factor of 230.

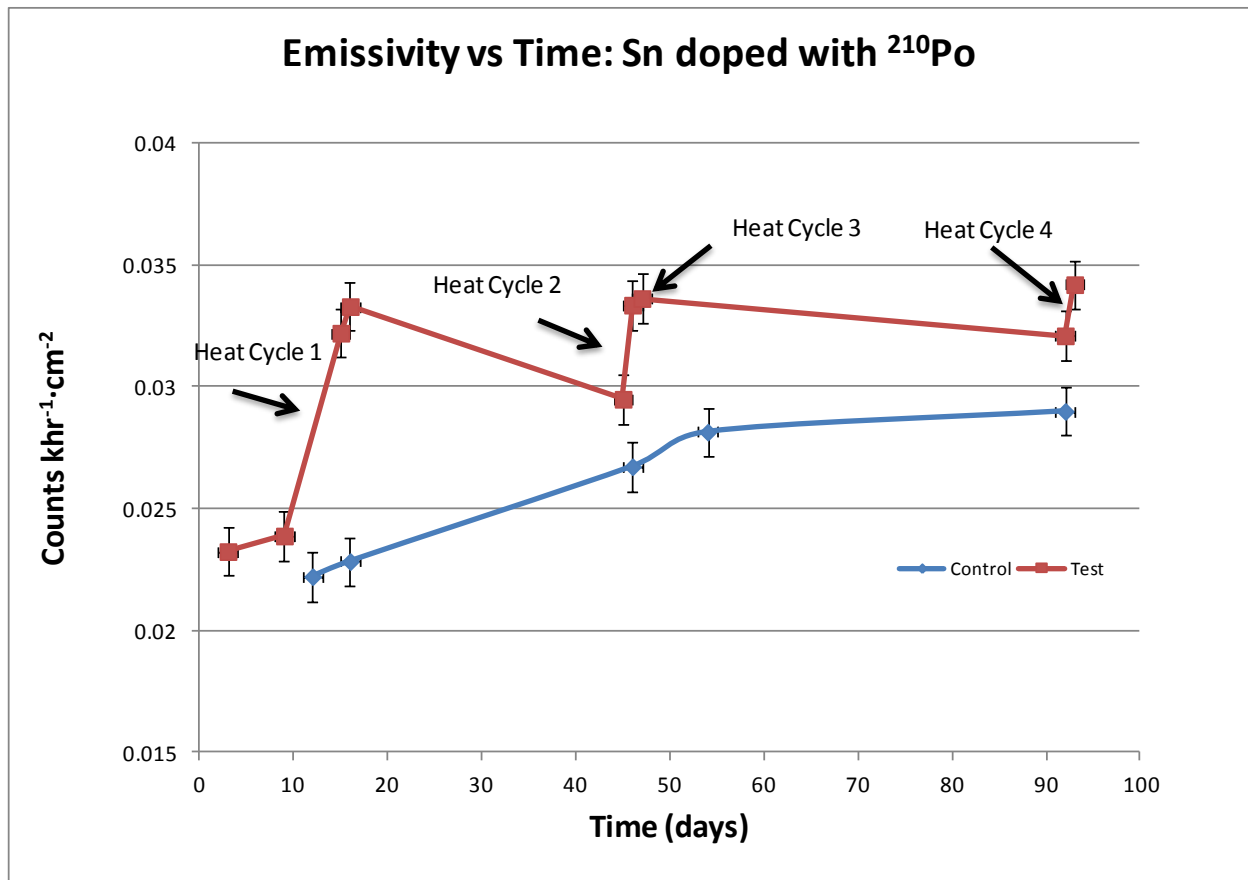


Figure 8. Alpha emissivity versus time for Sn doped with ²¹⁰Po.

Packaging Considerations

The implications for packaging applications using tin, tin alloys, or other metal materials are significant. Materials or structures undergoing phase transitions are susceptible to microsegregation, which may lead to incorrect certification to a specified alpha emissivity level because of emitter sequestration outside of the analytical volume. In addition, elevated temperature packaging processes will activate ^{210}Po diffusion to sensitive locations where the 5.3 MeV alpha has a larger cross section of initiating SEU.

The SEU risk from Po is unique and troublesome for two reasons. First, Po mobility within solid materials has the possibility to negate to some extent shielding effects assumed in IC designs by moving the emitter within range of vulnerable locations. Specifically, diffusion induced surface emission may cause an unexpected increase in SER if assumptions of volume emission and static emitter position are erroneous.⁴ Second, Po has the combination of high specific activity (alphas emitted per unit mass) and a high energy alpha particle. Therefore, a small number of atoms per unit area will result in a significant high energy alpha flux with an extended range in IC devices.

The secular equilibrium behavior of thin lead samples reported by Gordon⁴ indicate for processes like electroplating where microsegregation is not present, diffusion effects are minimal and secular equilibrium alone may be sufficient to explain

time dependent alpha emissivity. Microsegregation is not expected in material deposited by processes lacking phase transitions (i.e. electroplating, physical vapor deposition (PVD), or chemical vapor deposition (CVD)). However, if contaminants are present in the deposition processes at a sufficient level, it is conceivable that the diffusion mechanism could be active.

The mobility of Po also requires a fundamental shift in how alpha emissivity is viewed. Alpha emissivity has been assumed to be a volumetric quantity. However, diffusion drives Po to the surface, reducing alpha emissivity from a three dimensional quantity to a two dimensional quantity. In effect, diffusion acts to compress alpha emitters distributed in three dimensions into two, resulting in an areal density of emitters larger than the volume density of emitters. The 4π alpha emissivity as a function of sphere diameter was calculated for a hypothetical material with a Po concentration of 10^4 atoms per gram. The calculations assume 100% Po diffusion to the surface from an initial homogeneous distribution. This suggests that the alpha emissivity is determined by the absolute, and not relative, number of emitting atoms in the volume. As Figure 9 indicates, reducing the sphere volume leads to an exponential decrease in alpha emissivity.

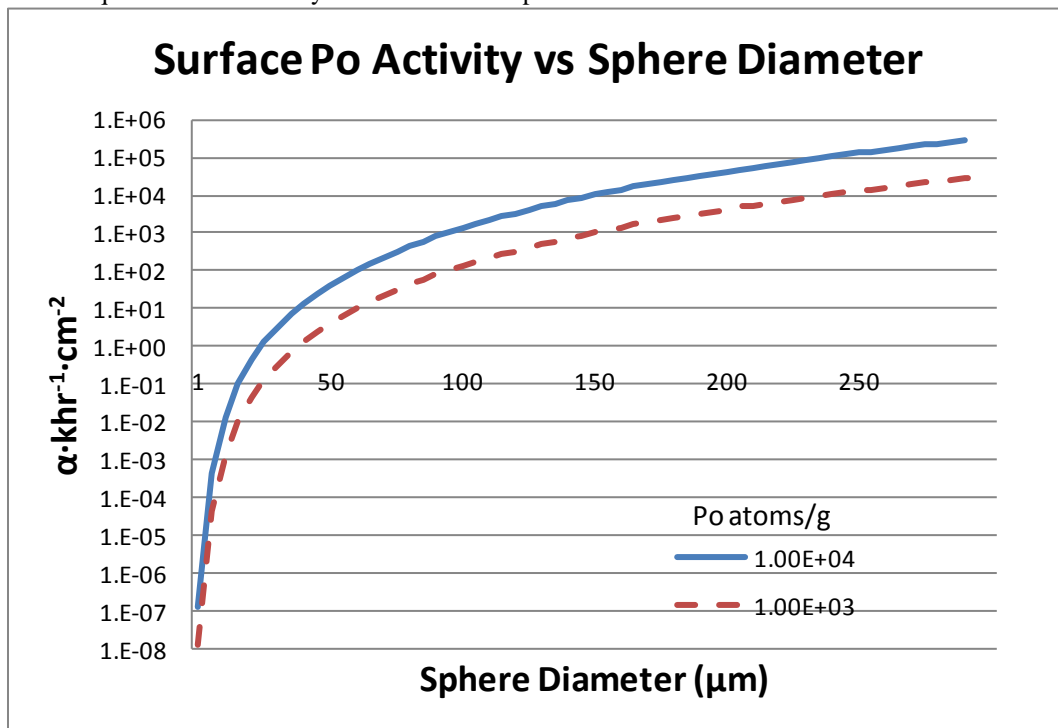


Figure 9. Sphere surface activity resulting from diffusion of 10^4 atoms Po/gram Sn.

While the cautions offered may cause some alarm, it should be noted that examples exist of Sn sufficiently pure that effects from either mechanism are not detectable (Sample A of experiment 1). These cases have sufficiently low contaminant concentrations that microsegregation is minimized, and the amount of ^{210}Po is less than measurement limits. The solution is to remove contaminants that are the root cause of the emission, specifically uranium, thorium, and the associated daughters. Refining process capability may be overstated due to microsegregation obscuring true material quality. To this end, Honeywell has developed proprietary refining processes specifically targeting these species.

Conclusions

The combination of microsegregation and diffusion provide a new basis to explain changes in alpha emissivity of materials. The data suggest that ^{210}Po is a key component in alpha emissivity dynamics. Processing can significantly affect position of alpha emitters in a material or structure, especially processes that involve liquid/solid phase transitions. The presence of microsegregation on a sub ppb concentration scale has been reported using direct alpha radiation measurements. In the case of alpha emissivity measurements, the impacts of small analytical volume need to be considered when extrapolating results across the entire volume. Heterogeneity effects on the results can be acute in such circumstances. This emphasizes an inherent limitation involving alpha measurements: analytical volume as a percentage of sample volume is potentially very small. Measurements made assuming near surface volume is representative of the entire sample volume will be erroneous if microsegregation effects are present.

Since nuclear decay is independent of chemical and physical state, any alpha emissivity increase as a function of temperature can be attributed Po diffusion. A static view of Po behavior is oversimplified in processes undergoing phase transitions and temperature variations. Transport of ^{210}Po has been quantitatively described, with the rate of diffusion driven by temperature. The dynamic nature of this potential problem underscores the importance of removing these species using specific refining strategies. Data presented demonstrate that material with sufficiently low impurities will be comparably stable over time with respect to alpha emissions.

The data reported confirm earlier published observations of Po accumulation on the surface of Sn and describe diffusion rates at room and elevated temperatures. The diffusion mechanism can play a

significant role in temporal alpha emissivity, and will be amplified to the extent that microsegregation effects are present. Secular equilibrium is expected to explain alpha emissivity in systems where these two mechanisms are absent. Polonium diffusion has been documented in both Sn and Pb.

In cases of Po diffusion, alpha emission is no longer an intensive property unrelated to the mass of the material. It has been experimentally demonstrated that essentially all Po present in a mass can be driven preferentially to the surface. The amount accumulating at the surface is directly proportional to the absolute amount present in the mass. Therefore, reducing packaging material mass will result in reduced alpha emissions.

Acknowledgements

The author wishes to acknowledge Michael Fields for GDMS analysis and Michael Paladin, Jack Long, and Thomas Ploegman for assistance with sample preparation.

Disclaimer

Although all statements and information contained herein are believed to be accurate and reliable, they are presented without guarantee or warranty of any kind, express or implied. Information provided herein does not relieve the user from the responsibility of carrying out its own tests and experiments, and the user assumes all risks and liability for use of the information and results obtained. Statements or suggestions concerning the use of materials and processes are made without representation or warranty that any such use is free of patent infringement and are not recommendations to infringe any patent. The user should not assume that all toxicity data and safety measures are indicated herein or that other measures may not be required.

References

- ¹ F. Wrobel,, F. Saigne, M. Gedion, J. Gasiot, R.D. Schrimpf, IEEE Transactions on Nuclear Science, Vol. 56, No. 6 pp. 3437-3441, December, 2009.
- ² D. F. Heidel, K. P. Rodbell, E. H. Cannon, C. Cabral Jr., M. S. Gordon, P. Oldiges, and H. H. K. Tang, "Alpha-particle-induced upsets in advanced CMOS circuits and technology," IBM J. Res. Dev., Vol. 52, No. 3, pp. 225–232, May, 2008.
- ³ B. M. Clark, M. W. Weiser, I. Rasiah, "Alpha Radiation Sources in Low Alpha Materials and

Implications for Low Alpha Materials Refinement”,
Thin Solid Films Vol. 462, pp. 384-386, 2004.

⁴ M. S. Gordon, K. P. Rodbell, D. F. Heidel, C. E. Murray, H. H. K. Tang, B. Dwyer-McNally, W. K. Warburton, Alpha Particle Emission Energy Spectra From Materials used for Solder Bumps, IEEE Transactions on Nuclear Science, Vol. 57, No. 6, pp. 3252-3256, December, 2010.

⁵ F. Wrobel, J. Gasiot, F. Saigne, “Hafnium and Uranium Contributions to Soft Error Rate at Ground Level”, IEEE Transactions on Nuclear Science, Vol. 55, No. 6, pp. 3141-3145, December, 2008.

⁶ M. Gedion, F. Wrobel, F. Saigne, M. Portier, A.D. Touboul, R.D. Schrimpf, “Effect of the Uranium Decay Chain Disequilibrium on Alpha Disintegration Rate”, IEEE Transactions on Nuclear Science, Vol. 58. No. 6, pp. 2793-2797, December, 2011.

⁷ JEDEC Standard 221Alpha Radiation Measurement in Electronic Materials

⁸ SRIM.com

⁹ H.D. Brody, “Microsegregation”, Casting, Vol 15, ASM Handbook, ASM International, 2008, p 338-347.

¹⁰ T. Kraft, Y.A. Chang, Journal of the Minerals, Metals and Materials Society Volume 49, Number 12 (1997), 20-28.

¹¹ F. Wrobel, F. Saigne, M. Gedion, J. Gasiot, R. D. Schrimpf, “Radioactive Nuclei Induced Soft Errors and Ground Level”, IEEE Transactions on Nuclear Science, Vol. 56, No. 6, pp. 3437-3441, December, 2009.

¹² M. S. Gordon, D. F. Heidel, K. P. Rodbell, B. Dwyer-McNally, W. K. Warburton, “An Evaluation of an Ultra-Low Background Alpha Particle Detector”, IEEE Transactions on Nuclear Science, Vol. 56, No. 6, pp. 3381-3386, December, 2009.

¹³ A. Zastawny, J. Bialon, T. Sosinski, “Migration of ²¹⁰Po in Lead to the Surface”, Appl. Radiat. Isot. Vol. 43 No. 9, pp.1147-1150, 1992.

¹⁴ G. Lykken, B. Momcilovic, “Preparation of Pb Thin Samples for Alpha Particle Emission Test”, US patent 6,674,072 January 6, 2004.